

SLAC-PUB-4746 Rev.  
June 1989  
(A)

**FINAL FOCUSING AND ENHANCED DISRUPTION FROM  
AN UNDERDENSE PLASMA LENS IN A LINEAR COLLIDER\***

P. CHEN, S. RAJAGOPALAN §

*Stanford Linear Accelerator Center*

*Stanford University, Stanford, California 94309*

J. ROSENZWEIG

*High Energy Physics Division,*

*Argonne National Laboratory, Argonne, Illinois 60439*

**ABSTRACT**

In this work we examine the viability of employing an underdense plasma lens as a final focusing method for a linear  $e^+e^-$  collider. The underdense plasma lens is superior to the overdense lens in that it improves focusing linearity and background event rate, but works well only for electrons. We thus consider the interaction of an  $e^-$  beam which is smaller than the  $e^+$  beam at collision, a case we term "bootstrap disruption". Potential luminosity enhancement is determined by analysis of the lens optics and simulation of the bootstrap disruption.

*Submitted to Phys. Rev. D*

---

\*Work supported by the Department of Energy, contracts DE-AC03-76SF00515, DE-AC03-88ER403A and W-31-109-ENG-38.

§Permanent address: Physics Dept, University of California, Los Angeles, CA 90024.

As the energy of circular colliding beam machines becomes higher, one must face the limitation imposed by the energy loss to synchrotron radiation. For this reason, it is likely that future lepton colliders will be linear machines. The disadvantage of the linear scheme is that the beams are used only once, and then discarded. In order to achieve desirable luminosity  $\mathcal{L} = f_{rep} N^2 H_D / 4\pi \sigma_0^{*2}$  where  $N$  is the number of particles per bunch,  $f_{rep}$  the collider repetition rate,  $H_D$  the beam-beam disruption enhancement factor and  $\sigma_0^*$  the rms beam radius at collision, one must either increase the beam current  $f_{rep} N$  or decrease the spot size. The current is constrained by many factors, e.g. power limitations, wake-field effects. On the other hand, the minimum spot sizes are presently limited by the strength of conventional focusing quadrupoles. Clearly, much is to be gained by achieving smaller beam spot sizes.

The plasma lens, which uses the self-focusing wake-fields of a bunched relativistic charged particle beam in a plasma, has been recently discussed as a candidate for a luminosity-enhancing linear collider final focus system.<sup>1-5</sup> Confirmation of the existence of strong focusing in plasma wake-fields has been experimentally verified in tests performed at Argonne Advanced Accelerator Test Facility.<sup>6,7</sup> The experimental and theoretical work to date has concentrated mainly on the overdense plasma lens, where a beam whose peak density  $n_b$  is much less than the ambient plasma density  $n_0$  it encounters as it traverses the lens. In this case assuming that the beam length  $\sigma_z$  is large compared to the plasma wavelength  $\lambda_p = \sqrt{\pi r_e / n_0}$  (the response of the plasma electrons to the beam is adiabatic and not oscillatory), the beam width  $\sigma$  is small compared to the plasma wavelength (plasma response is radial), and the ions are stationary, then the plasma electrons move to approximately neutralize the beam charge, leaving the beam current self-pinching forces

unbalanced (see Refs. (1)–(4) for a thorough discussion of the linear plasma fluid theory involved). In this case the focusing wake-fields reduce, to a good approximation, to the magnetic self-fields of the beam.

These self-fields are quite strong, but as they are dependent on the configuration of the beam density, the resulting focusing is nonlinear and aberration prone. This requires that the lens be placed very close to the interaction point to minimize aberration effects, which in turn means that, for parameters typical of the Stanford Linear Collider (SLC) design, the plasma lens must be very dense. This dense plasma is a source of a very large background event rate. For instance, using the lens design analysed in Ref. (3), we have a fully ionized hydrogen plasma of density  $n_0 = 5 \times 10^{18} \text{ cm}^{-3}$ , length 3 mm, focal length 1 cm, and  $e^-(e^+)$  bunches with  $N = 5 \times 10^{10}$  particles. The inelastic scattering cross section for a 50 GeV electron incident on a stationary proton is calculated to be 34  $\mu\text{barns}$  in the resonance region, i.e., final state mass below 2 GeV, and 14  $\mu\text{barns}$  above 2 GeV. Thus the background rate due to e-p inelastic scattering is of the order of a few per beam crossing. This seems incompatible with unambiguous high energy experiments in a linear collider.

The background and aberration problems motivate the investigation of the underdense plasma lens. In this regime, the beam is denser than the plasma, and the plasma response is not described well by linearized fluid theory. An underdense plasma reacts to an electron beam by total rarefaction of the plasma electrons inside the beam volume, producing a uniformly charged ion column of charge density  $en_0$ . This uniform column produces linear, nearly aberration-free focusing. Simulations have shown that one needs to have  $n_b \geq 2n_0$  to produce linear focusing over most of the bunch.<sup>8</sup> This scheme for employing plasma focusing is also sometimes

termed the ion focusing regime (IFR), and has been used for transporting low energy, intense relativistic electron beams.<sup>9</sup> For positron beams, however, plasma electrons do not behave simply, and the focusing is not linear. For this reason, we concentrate mainly on the optics of the electron beam in the underdense lens and then examine the luminosity enhancement achieved by the disruption of the larger positron beam by the smaller electron beam. We term this process bootstrap disruption, as it involves a cascade of beam-dependent focusing effects; the pre-focusing of the electron beam by its own self-fields and the subsequent strengthened disruption of the positron beam by the electron beam.

We begin our analysis by examining the third-order linear differential equation for the beam  $\beta$ -function as a function of the distance down the beam-line  $s$

$$\beta''' + 4K\beta' + 2K'\beta = 0 \quad , \quad (1)$$

where  $\beta = \sigma^2/\epsilon_0$ ,  $\epsilon_0$  is the unnormalized transverse emittance and  $K = 2\pi r_e n_0/\gamma$  is the focusing strength of the lens. To solve Eq. (1) we must first integrate through the  $\delta$ -function in  $K'$  at the start of the lens to obtain  $\Delta\beta_0'' = -2K\beta_0$ . The other two initial conditions are just continuity requirements  $\beta' = \beta_0'$ , and  $\beta = \beta_0$ . Assuming the electron bunch to have a cylindrically symmetric bi-Gaussian distribution of rms length  $\sigma_z$ , then we can define the phase space density parameter  $\zeta = Nr_e/\sqrt{8\pi}\epsilon_0\gamma\sigma_z$ , and the focusing strength of an underdense plasma lens is, with  $\beta = \beta_0$  and  $n_0/n_b = 1/2$  at the start of the lens,  $K = \zeta/\beta_0$ . Using the initial conditions we integrate Eq. (1) once to obtain

$$\beta'' + 4K\beta = 2/\beta_0^* + 2\zeta \quad , \quad (2)$$

where  $\beta_0^*$  is the minimum  $\beta$ -function achieved in the absence of the plasma lens.

The solution for the  $\beta$ -function inside the lens is easily found from Eq. (2) to be

$$\beta = \frac{\beta_0}{2} + \frac{1}{2K\beta_0^*} + \left(\frac{\beta_0}{2} - \frac{1}{2K\beta_0^*}\right) \cos \nu(s - s_0) + \frac{2s_0}{\nu\beta_0^*} \sin \nu(s - s_0) \quad , \quad (3)$$

where  $\nu^2 = 4K$ .

It is straightforward to show from the above considerations that the maximum reduction in  $\beta^*$  that one can achieve with this lens occurs when one places the entrance of the plasma at a position  $-s_0 \gg \beta_0^*$ . This reduction is given by

$$\frac{\beta^*}{\beta_0^*} = \frac{1}{1 + K\beta_0^*(\beta_0 - \beta_1)} \simeq \frac{1}{1 + \zeta\beta_0^*} \quad (4)$$

where  $\beta_1$  is the  $\beta$ -function at the exit of the plasma lens at  $s = s_1$ . For SLC design parameters ( $\epsilon_n = 3 \times 10^{-5}$  mrad,  $\sigma_z = 1$  mm,  $\beta_0^* = 7$  mm,  $\gamma = 10^5$ , and  $N = 5 \times 10^{10}$ ) we have  $\zeta = 9.4 \times 10^2 \text{ m}^{-1}$ , and a possible reduction in  $\beta$  of 1/7.5.

It is also interesting to note that according to this formula, one should never back off of the focus, i.e., make  $\beta_0^*$  larger, as the ultimate  $\beta^*$  attainable is inversely proportional to  $\zeta + (1/\beta_0^*)$ . This implies one should minimize  $\beta_0^*$ . It also says that if  $\zeta\beta_0^* < 1$  then plasma lens is irrelevant, as it is not strong enough to overcome the inherent divergence in the beam. If one only reduces the spot size  $\sigma_-^*$  of the electron beam in the collisions and leaves the positron beam spot size  $\sigma_0^*$  unchanged, then the possible luminosity enhancement due to the lens  $H_L$  (excluding depth of focus and disruption effects) is easily shown to be

$$H_L = \frac{2(\sigma_0^*)^2}{(\sigma_-^*)^2 + (\sigma_0^*)^2} = \frac{2\beta_0^*}{\beta_-^* + \beta_0^*} \quad , \quad (5)$$

which is strictly less than two. For example, an electron spot size reduction of  $\sigma_-^*/\sigma_0^* = 0.4$  gives a luminosity enhancement of 1.73. This is a very modest number; it is boosted, however, by the bootstrap disruption enhancement.

Previous calculations of the luminosity enhancement due to beam-beam disruption have treated symmetric beams. It has been found<sup>10</sup> that the disruption luminosity enhancement is influenced by two factors: the strength of the pinch, represented by the disruption parameter  $D$ ,

$$D = \frac{Nr_e\sigma_z}{\gamma\sigma_0^{*2}} = \frac{Nr_e\sigma_z}{\gamma\beta_0^*\epsilon_0} \quad , \quad (6)$$

and the effects of the inherent divergence of the beam, represented by the parameter  $A = \sigma_z/\beta_0^*$ . The disruption enhancement is a strongly decreasing function of  $A$  when  $A > 1$ , due to the effects of depth of focus and inherent beam divergence, and a monotonically increasing function of  $D$ . Since both  $D$  and  $A$  are inversely dependent on  $\beta_0^*$ , there exists a maximum luminosity for some value of  $\beta_0^*$ . We will also see this effect in bootstrap disruption calculations.

To study the process of bootstrap disruption we employ the particle-in-cell computercode ABEL, developed by K. Yokoya<sup>11</sup> and modified for our purposes to handle unequal spot size beam collisions. The code simulates the interaction of two beams which have Gaussian profiles in all five active phase space dimensions:  $x, x', y, y', z$ . The fields are calculated from the assumption of cylindrical symmetry. The effects of synchrotron radiation energy loss (beamstrahlung) are ignored.

In the case of equal spot sizes, the relevant parameter space for disruption enhancement is only two-dimensional ( $D, A$ ) and some very general results have been obtained which map out this parameter space well.<sup>10</sup> With unequal spot sizes the parameter space becomes four-dimensional and a bit unmanageable to study in general terms. We therefore concentrate on cases which are interesting for SLC-type parameters. We examine two cases, one corresponding to SLC Phase I in which

the conventional final focus  $\beta_0^* = 7$  mm (with conventional final quadrupoles), and the SLC Phase II with  $\beta_0^* = 5$  mm (superconducting final quadrupoles). Calculations were performed with the positrons undergoing the conventional focus and the electrons undergoing an aberration-free focus in the underdense plasma lens. Note that for  $\beta_0^* = 7$  mm the minimum electron spot size achievable with the underdense lens is  $\sigma_-^*/\sigma_0^* = 1/\sqrt{7.5}$ , and for  $\beta_0^* = 5$  mm is  $\sigma_-^*/\sigma_0^* = 1/\sqrt{5.7}$ .

In Fig. 1 we plot the luminosity enhancement including bootstrap disruption effects  $H_B$  using SLC-type design parameters, from focusing only the electron beam, as a function of relative electron beam spot size  $\sigma_-^*/\sigma_0^*$ . Note that the process saturates below approximately  $\sigma_-^*/\sigma_0^* = 0.4$  for both values of  $\beta_0^*$ , 7 mm and 5 mm. The case of  $\beta_0^* = 7$  mm saturates at a higher luminosity enhancement of  $H_B \simeq 2.9$ , as the  $\beta_0^* = 5$  mm case displays the negative effects of the larger inherent divergence in the beam. Note that the bootstrap enhancements in either case can exceed the naive geometrical limit of two. An underdense plasma lens that achieves  $\sigma_-^*/\sigma_0^* = 0.4$  can be easily designed by the use of Eq. (3). If one places a plasma of density  $n_0 = 1.5 \times 10^{15} \text{ cm}^{-3}$ , occupying the region between 5 and 10 cm from the desired interaction point, and initially tunes the electron beam to focus 10 cm downstream from the interaction point ( $s = -20$  cm) then the correct compression of the electron beam is obtained. This configuration allows the plasma to be entirely outside of the SLD vertex detector. Also, the integrated target density for backgrounds in this underdense lens scheme is  $n_0 l = 7.5 \times 10^{15} \text{ cm}^{-2}$ , in contrast to  $n_0 l = 3 \times 10^{18} \text{ cm}^{-2}$  for the overdense case discussed previously. Thus, the background event rates can be reduced by a factor of 400, which makes the lens much more attractive.

As the number of particles per bunch is increased, one expects the luminosity to increase by a rate greater than  $N^2$ , as the disruption enhancement monotonically increases with  $N$ . We wish to examine possible changes in this scaling in the presence of an underdense plasma lens and bootstrap disruption. In Fig. 2 we show the luminosity for our SLC parameter example, varying  $N$  from  $3 \times 10^{10}$  to  $7 \times 10^{10}$ . Two sets of curves are shown, corresponding to the cases with (solid line) and without (dashed line) an underdense plasma lens which focuses the electron beam down to  $\sigma_-^*/\sigma_0^* = 0.4$ . Since it is often difficult to obtain as large an  $N$  as one would like it is interesting to note that one can obtain the design luminosity associated with  $N = 5 \times 10^{10}$  and  $\beta_0^* = 7$  mm by using an underdense plasma lens for the electron beam and only two-thirds of the current. In Fig. 3 we show the actual luminosity enhancement due to the bootstrap disruption for these cases. We observe that the effect is nearly independent of  $N$  over the range of interest, with  $H_B \simeq 2.6 - 2.9$ .

Since simulations have shown that the underdense plasma lens can focus positrons, albeit with strong aberrations, it is interesting to see what sort of luminosity enhancements are ultimately possible using two underdense lenses. A theory of aberration-prone focusing is developed in Ref. (3), and we adopt some of these results, as well as computational results from Ref. (8), in simulating approximate cases. In terms of the quantity termed the aberration power  $P$ , the transformations of the initial transverse phase space parameters  $(\alpha_0, \beta_0, \epsilon_0)$  by an aberration prone thin lens are

$$\alpha = (\alpha_0 + \beta_0/f)/P, \quad \beta = \beta_0/P, \quad \epsilon = \epsilon_0 P \quad , \quad (7)$$

where  $f$  is the lens focal length,  $\alpha = -2\beta'$ , and  $P = \sqrt{1 + (\beta_0\delta/f)^2}$ .



The parameter  $\delta$  corresponds to the rms variation of the focusing strength  $K$  in the lens. Simulations have shown that for a mildly underdense lens that  $\delta \simeq 0.28$  for positron focusing. Note that in this model the aberration effects an emittance blowup which is dependent on the strength of the lens. The total reduction in spot size is thus.

$$\frac{\sigma^*}{\sigma_0^*} = \left[ \frac{\beta^* \epsilon}{\beta_0 \epsilon_0} \right]^{1/2} = \frac{P}{\sqrt{P^2 + (\alpha_0 + \beta_0/f)^2}} \quad (9)$$

Using this model we can simulate the collision of an electron beam focused by an underdense plasma lens to 0.4 of its original spot size with a positron beam focused, with aberrations, by a mildly underdense plasma lens. The luminosity obtained in this scheme is shown in Fig. 4 as a function of relative spot size of the positron beam, with all other parameters taken from SLC design. If one focuses the positrons to 0.6 of the conventionally achieved spot size then the luminosity is  $1.5 \times 10^{31} \text{ cm}^{-2} \text{ sec}^{-1}$  and (see Fig. 2) the total enhancement is approximately five. The physical parameters involved in this configuration are shown in Table 1. This treatment of the positron focusing is approximate, but gives qualitative insight into the role aberrations play in this scheme. Further computational study of the positron beam-underdense plasma interaction is necessary to form a more complete picture.

In conclusion, we have analysed the optics of the underdense plasma lens and addressed the bootstrap disruption by computer simulation. This investigation indicates that the luminosity enhancement factors of three to five may be possible above conventional focusing schemes for the SLC design parameters, with large reductions in background event rates from similar overdense plasma lens schemes.

The authors would like to acknowledge help in coding from K. Socha of Reed College.

## REFERENCES

1. P. Chen, *Particle Accelerators* **20**, 171 (1987).
2. P. Chen, J.J. Su, T. Katsouleas, S. Wilks, and J.M. Dawson, *IEEE Trans. Plasma Sci.* **PS-15**, 218 (1987).
3. J.B. Rosenzweig and P. Chen, SLAC-PUB-4571, 1988, to be published in *Phys. Rev. D*.
4. J.B. Rosenzweig, B. Cole, D.J. Larson, and D.B. Cline, in *Linear Collider  $B\bar{B}$  Factory Conceptual Design*, Donald H. Stork, ed., 346 (World Scientific, 1987) also to be published in *Particle Accelerators* (1988).
5. D. B. Cline, B. Cole, J. B. Rosenzweig and J. Norem, *Proceedings of the 1987 Washington Accelerator Conference*, 241 (IEEE, Washington, 1987).
6. J. Rosenzweig, D. Cline, B. Cole, H. Figueroa, W. Gai, R. Konecny, J. Norem, P. Schoessow and J. Simpson, *Phys. Rev. Lett.* **61**, 98 (1988).
7. J. Rosenzweig, B. Cole, W. Gai, R. Konecny, J. Norem, P. Schoessow and J. Simpson, Argonne Preprint ANL-HEP-PR-88-43 (August 1988), submitted to *Phys. Rev. Lett.*
8. J.J. Su, T. Katsouleas, J. Dawson, and R. Fedele, UCLA Preprint PPG (September 1988), submitted to *Phys. Rev. A*.
9. B. Hui and Y.Y. Lau, *Phys. Rev. Lett.* **53**, 2024 (1984).
10. P. Chen and K. Yokoya, *Phys. Rev. D* **38**, 987 (1988).
11. K. Yokoya, KEK Report 85-9, 1985 (unpublished).

TABLE 1. A Set of Plasma Lens Parameters for SLC

Plasma Lens Parameters	Electrons	Positrons
$n_0[\text{cm}^{-3}]$	$1.5 \times 10^{15}$	$4.8 \times 10^{16}$
$l[\text{cm}]$	5.0	0.33
Beam parameters		
$N$	$5 \times 10^{10}$	$5 \times 10^{10}$
$E[\text{GeV}]$	50	50
$\epsilon_0[\text{mrad}]$	$3 \times 10^{-10}$	$3 \times 10^{-10}$
$\sigma_z[\text{mm}]$	1.0	1.0
Beam Optics Parameters		
$s_0[\text{cm}]$	20.0	1.3
$\beta_0^*[\text{mm}]$	7.0	7.0
$\epsilon[\text{mrad}]$	$3 \times 10^{-10}$	$4.2 \times 10^{-10}$
$\beta^*[\text{mm}]$	1.12	1.84
$\delta$	0	0.28
$P$	1.0	1.39
$f[\text{cm}]$	7.5	1.1
Luminosity Enhancement		
$\mathcal{L}_{00}[10^{30}\text{cm}^{-2}]$	1.76	
$H_D$	1.73	
$\mathcal{L}_0(= H_D \mathcal{L}_{00})[10^{30}\text{cm}^{-2}]$	3.0	
$\sigma_{\pm}^*/\sigma_0^*$	0.4	0.6
$H_B$	5.0	
$-\mathcal{L}(= H_B \mathcal{L}_0)[10^{30}\text{cm}^{-2}]$	15.0	

## FIGURE CAPTIONS

- Fig. 1. Luminosity enhancement including disruption effects  $H_B$  using SLC-type design parameters, from focusing only the electron beam as a function of relative electron beam spot size  $\sigma_-^*/\sigma_0^*$ . Squares indicate  $\beta_0^* = 7$  mm, crosses  $\beta_0^* = 5$  mm.
- Fig. 2. Luminosity for SLC-type design parameters as a function of particle number  $N$ , with (solid line) and without (dashed line) an underdense plasma lens which gives  $\sigma_-^*/\sigma_0^* = 0.4$ .
- Fig. 3. Luminosity enhancement including bootstrap disruption as a function of particle number  $N$ , with  $\sigma_-^*/\sigma_0^* = 0.4$  from underdense plasma lens.
- Fig. 4. Luminosity for SLC-type design parameters as a function of relative positron beam size  $\sigma_+^*/\sigma_0^*$ , with focusing obtained from aberration-prone plasma lens. Electron beam is focused to  $\sigma_-^*/\sigma_0^* = 0.4$ .

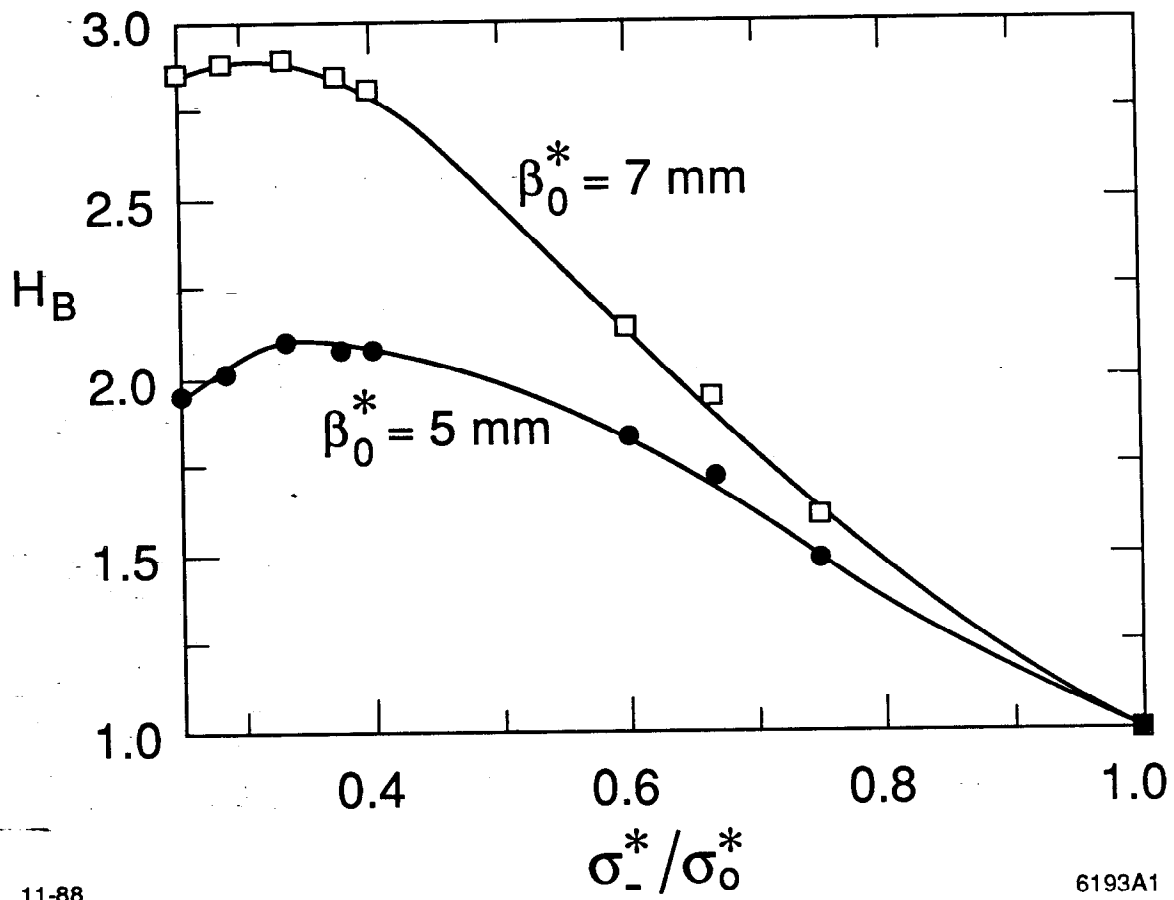
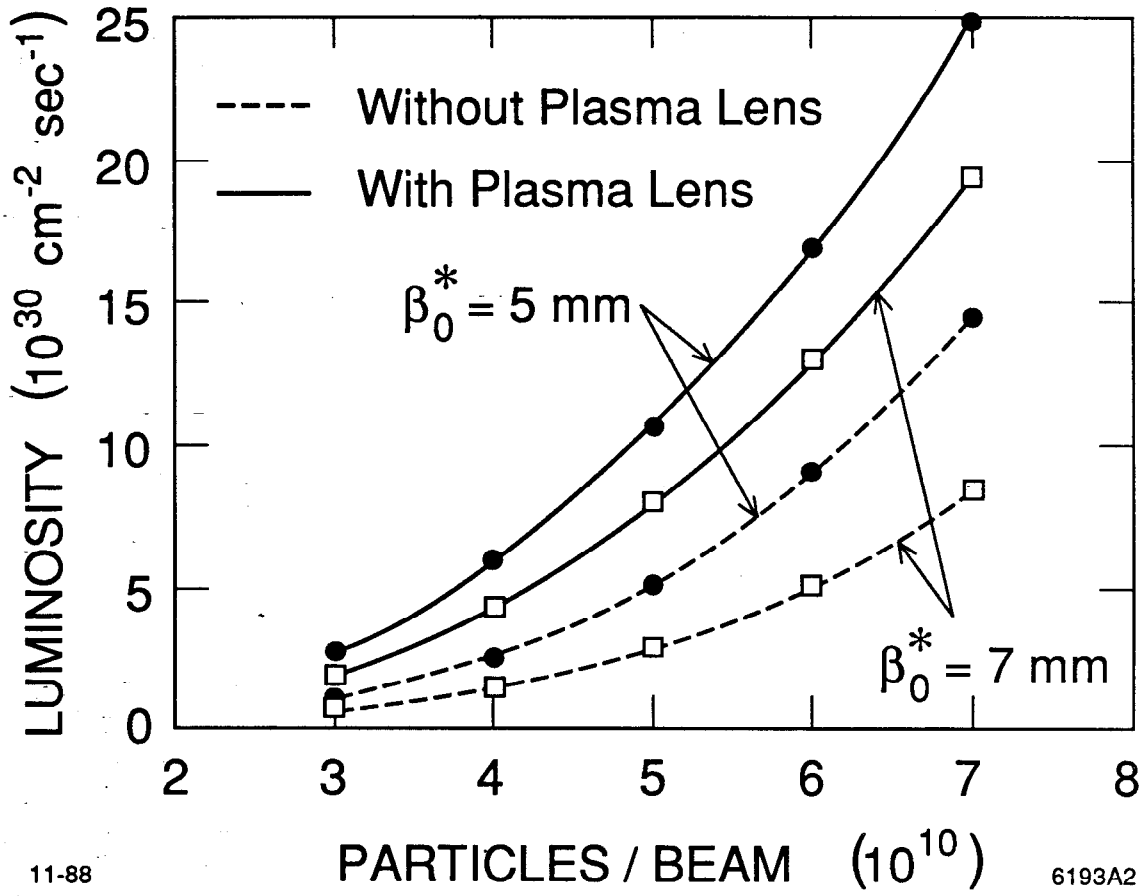


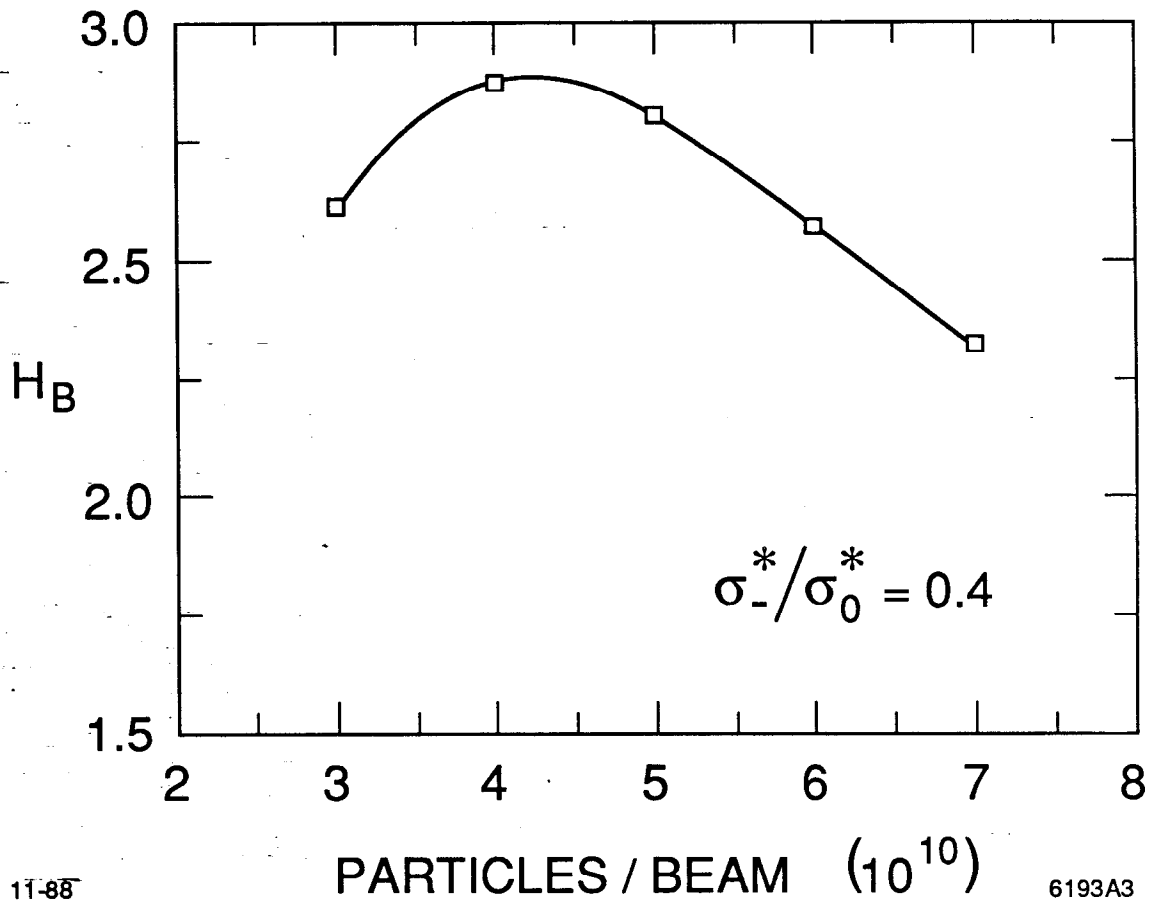
Fig. 1



11-88

6193A2

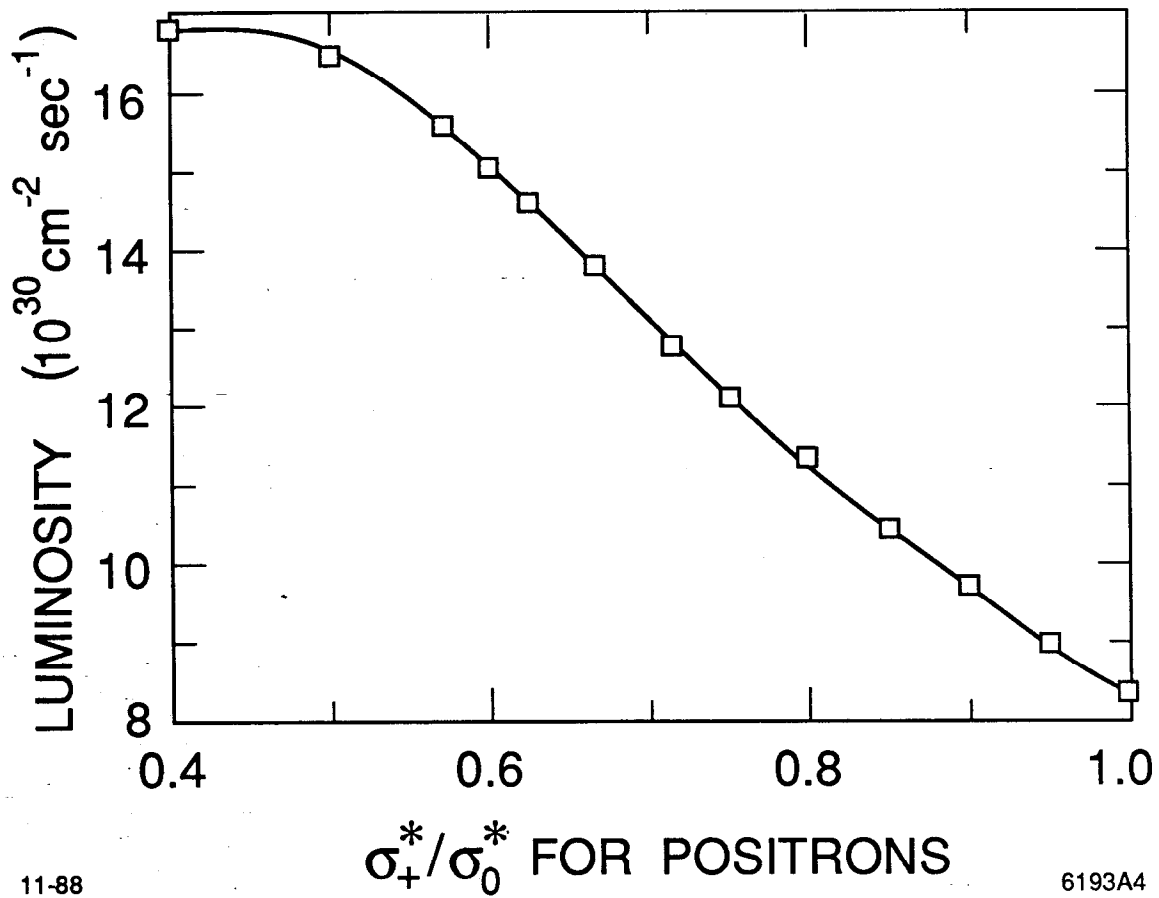
Fig. 2



11-88

6193A3

Fig. 3



11-88

6193A4

Fig. 4